Modeling and Control of Oxygen Transfer in High Purity Oxygen Activated Sludge Process

Chwen-Jeng Tzeng[1]; Reza Iranpour[2]; and Michael K. Stenstrom; F.ASCE[3]

Abstract: A dynamic mathematical model for the high purity oxygen activated sludge process, which incorporates structured biomass, gas–liquid interactions and control systems, was developed. The model was calibrated using pilot plant data associated with the development of the West Point Treatment Plant near Seattle, Wash. The calibrated model was used to simulate oxygen transfer rates for various operating conditions. Simulations showed that an optimal control system can reduce aerator power by 33% as compared to a conventional design, and reduce average oxygen feed gas by as much as 18%. Vent gas purity control dramatically reduced the peak aerator horsepower required to maintain set point dissolved oxygen concentration during high loadings. Step feed operation reduced the stag-to-stage variation in aerator horsepower and also reduced the required peak power. Predicted power savings for a 605,000 m^3/day plant were $500,000 per year at current power costs.

DOI: 10.1061/(ASCE)0733-9372(2003)129:5(402)

CE Database subject headings: Activated sludge; Aeration; Oxygen; Mathematical models; Oxygen transfer; Simulation; Wastewater.

Introduction

The West Point Treatment Plant (WPTP) was formerly a primary treatment plant operated by the Municipality of Metropolitan Seattle (Metro) and was upgraded to secondary treatment using high purity oxygen activated sludge (HPO-AS) technology. The plant has been operating successfully for several years. A dynamic mathematical model, incorporating carbonaceous substrate removal, secondary clarification, various control techniques, and gas–liquid mass balances, was developed for use as a tool for designing the plant and developing control strategies.

In order to maintain an enriched oxygen gas-phase and economize its use, the HPO-AS process uses covered aeration tanks-in-series. Four to six aeration tanks are typically used in series, and large plants use several parallel trains of tanks-in-series. This makes the process more complex and difficult to model and control compared to an air AS process. Oxygen consumption, carbon dioxide production, and nitrogen stripping create varying gas composition in the reactors, which requires the model to include gas phase material balances and gas–liquid phase interactions.

The gas–liquid interactions present challenges as well as opportunities. Molecular oxygen is consumed while carbon dioxide is produced and nitrogen is stripped from the influent. The net production and stripping of gases is always smaller than oxygen consumption, which means gas flow decreases through the stages. Changes in gas phase composition affect the aeration capacity of the process as well as mixed-liquor pH. Unlike air AS, design engineers and operators have two options in achieving oxygen transfer rates: aerator power and oxygen purity. The combination of the two present more flexibility; high loads can be treated by using maximum aerator power and lower oxygen purities, or lower aerator power and maximum oxygen purity. Automatic control systems can be used to manipulate oxygen purity and aerator power in combination to minimize total power or cost.

The model was originally developed to assist with the design of the Westpoint Treatment plant in Seattle, Wash. (Stenstrom 1990). It was calibrated using pilot plant data specifically obtained for constructing the new plant (Samstag et al. 1989). Various control strategies and design alternatives were developed afterward and are presented in this paper. The results are not the same as the final plant design, since various plant changes were made during construction and after startup. The control strategies described in this paper were not part of the design project. The overall results of this paper are a useful exercise in sizing HPO-AS plants for various conditions and demonstration of alternatives available to design engineers.

The model is dynamic and divides influent substances into five different pools. Among the five pools, two of them are biodegradable materials which follow different pathways as they are converted to cell biomass and final products. Thirteen kinetic parameters were calibrated using the pilot plant data. The model estimates oxygen requirements and determines the required aerator horsepower based on various influent conditions. Various ways of meeting peak loadings were evaluated, including control systems to manipulate HPO gas feed rate, aerator power, and step feed operation.

Plant Description

The full-scale design has four stages in each aeration train and six parallel trains. The design flow rate varies from 605,000 m^3/day

[1]Section Chief, China Engineering Consultants, Inc., 21FL, 185 Hsin-Hai Rd., Taipei, Taiwan 10637.

[2]Head, Hyperion Applied Research Group, Bureau of Sanitation, Hyperion Treatment Plant, 12000 Vista del Mar, Playa Del Rey, CA 90293.

[3]Professor, Civil and Environmental Engineering Dept., Univ. California Los Angeles, 5714 Boelter Hall, Los Angeles, CA 90095-1598 (corresponding author). E-mail: stenstro@seas.ucla.edu

Note. Associate Editor: Bruce Ernest Logan. Discussion open until October 1, 2003. Separate discussions must be submitted for individual papers. To extend the closing date by one month, a written request must be filed with the ASCE Managing Editor. The manuscript for this paper was submitted for review and possible publication on December 26, 2001; approved on April 11, 2002. This paper is part of the ***Journal of Environmental Engineering***, Vol. 129, No. 5, May 1, 2003. ©ASCE, ISSN 0733-9372/2003/5-402–411/$18.00.

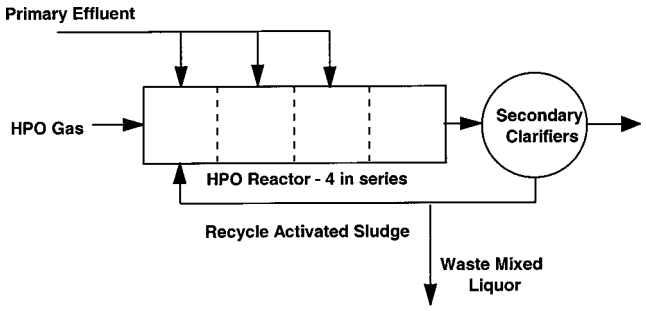

Fig. 1. Schematic of secondary portion of plant

(159 MGD) average to 1,130,000 m^3/day (300 MGD) peak flow rate with different seasonal loadings for the projected year 2005. The proposed HPO feed oxygen gas purity is 97%. Treatment goals are secondary standards [30 mg/L 5-day biological oxygen demand (BOD_5) and 30 mg/L total suspended solids], and nutrient removal is not required. Various maximums and peaking factors are required and are discussed later when they are simulated.

One special aspect of this design compared to other HPO processes is that any percentage of the influent flow can be distributed to each stage (i.e., step feed). This option was provided because of the extremely poor settling characteristics demonstrated by pilot plant results. The special case where 100% of the influent flow enters stage 2 was emphasized in this study. The purpose of the ''reaeration mode'' is to provide better sludge bulking control. Fig. 1 is a schematic of the secondary portion of the plant. Table 1 shows the nominal process sizes.

Model Development

Several steady state models have been previously developed for the HPO-AS process. (Mueller et al. 1973; McWhirter and Vahldieck 1978; Linden 1979). Clifft and Andrews (1986) and Clifft and Barnett (1988) modeled process control strategies for HPO-AS using a dynamic model. Stenstrom et al. (1989) developed a dynamic model using a single biomass and substrate model and showed how it could be used to describe the Sacramento Regional Treatment Plant and its performance during warranty testing. The model proposed here uses a very similar approach to our earlier work, except that a structured biomass is used. The gas transfer model is also similar.

Oxygen Transfer

The major difference between the HPO-AS process and air AS is the oxygen transfer rate. The rate of oxygen transfer can be estimated by the broadly accepted two-resistance theory. The overall mass transfer coefficient based on the overall concentration difference is expressed as follows [Mueller et al. 1973; American Society for Civil Engineers (ASCE) 1991]:

$$\frac{\mathrm{dDO}}{\mathrm{d}t} = \alpha K_L a(\mathrm{DO}_\infty^* - \mathrm{DO}) \tag{1}$$

where $K_L a$ = overall mass transfer coefficient (h^{-1}); DO = dissolved oxygen concentration (mg/L); DO_∞^* = equilibrium DO concentration (mg/L); and α = alpha factor, ratio of process water to clean water $K_L a$'s.

The average real-time DO concentration is approximately 0.5–3.0 mg/L for a conventional AS process, and 4–8 mg/L for an HPO process (McWhirter and Vahldieck 1978). The saturation or equilibrium DO concentration is proportional to the partial oxygen pressure, and is calculated using Henry's law. Therefore at 97% oxygen purity, the equilibrium concentration would be 4.64 times greater (97%/20.9%) than in atmospheric air. The mass transfer coefficient $K_L a$ is not a function of oxygen partial pressure, and the overall oxygen transfer rate is directly proportional to the driving force. Therefore the equipment used in an HPO-AS, as compared to an air AS, should transfer oxygen at a ratio approximately equal to overall ratios of the oxygen partial pressure. Transfer of carbon dioxide and nitrogen are modeled in the same fashion. The $K_L a$s for nitrogen and carbon dioxide are set to the square root of the ratios of their molecular diffusivities to oxygen diffusivities. The square root (penetration or surface renewal theory) was selected over the simple ratio (two film theory). Empirically, powers between 0.5 and 1.0 have been measured for different turbulence levels, Henry's constants, aeration system type, and ratio of gas film to liquid film resistance (Hsieh et al. 1993a, b) Surface renewal theory was selected because the system is highly turbulent, although the simulation results are not particularly sensitive to the power, at least for these conditions.

Biological Oxidation

The previous model developed for HPO-AS by our group was based upon Monod kinetics and used an unstructured biomass (Stenstrom et al. 1989). In this research, activated sludge process modifications such as step feed, were evaluated, which required a

Table 1. Nominal Process Size

Parameter	Value	Total per train	Total plant
Stages	17.1 m L × 17.1 m W × 7.6 m SWD	4	24
Stage liquid volume	2,200 m^3	8,800 m^3	53,200 m^3
Stage head space volume	355 m^3	1,420 m^3	8,520 m^3
Aerator power (stages 1–4)	56,93,93,56 kW (75,125,125,75 horsepower)	298 kW (400 horsepower)	1,788 kW (2,400 horsepower)
Clarifier area	43.4 m diameter 1478 m^2 4.9 m SWD		13 clarifiers 19,221 m^2
Recycle rate	50%		
Temperature	15°C		

structured model. The structured biodegradation approach divides the organic compounds and biomass into active and inactive pools in order to provide a more realistic simulation.

Substrate transfers very quickly from the liquid phase to the floc phase (Heukelekian 1941), and this transfer rate is much more rapid than the rate at which the substrate is metabolized by the floc. The specific growth rate and the concentration of substrate in the liquid does not always control growth rate, and it is suggested that the specific growth rate may be mostly dependent on the amount of limiting substrate within the floc. Unstructured models cannot be expected to predict accurately the dynamics of oxygen utilization because they are not capable of predicting the lag in organism growth rate that is observed in practice with increasing substrate concentration.

The structured biodegradation model proposed by Busby and Andrews (1975); Stenstrom and Andrews (1979); and Clifft (1980) predates the now widely accepted IAWQ 1 ASP model (IAWQ 1986), but has similar concepts. The influent is divided into four major pools: soluble substrate, particulate substrate, biologically inert mass, and nonvolatile mass. Among the four pools, only soluble substrates and particulate substrates are biodegradable. The ability of bacterial cells to store nutrients when the food to microorganism ratio is high and to use these stored materials when food is less abundant is a well-known mechanism that has been experimentally verified (e.g., Jacquart et al. 1972). Soluble substrates follow two different pathways where it is broken down and used to produce new cells. It can either be metabolized directly or converted to stored mass. The definition of stored mass here includes suspended and colloidal biodegradable organic materials that become enmeshed in the floc phase. The steps in biodegradation and cell decay are similar to the IAWQ model but different in one important way. In this model, cells decay to carbon dioxide, water, and inert mass while consuming oxygen. In the IAWQ model, a portion of biomass from cell decay is converted to inert mass and the rest is returned to the substrate pool, and no oxygen is consumed. Pathway f5 in Fig. 2 is different in the IAWQ model, with a portion $(1-Y_2)$ of the carbon associated with decaying cells returning to substrate. More detailed information is available (Yuan et al. 1993; Yuan 1994). The model is shown in Fig. 2, and the kinetic rate equations that correspond to the pathways are as follows:

$$f_1 = \text{bsstor} C_{\text{act}} S (f_{\text{cstorm}} - f_{\text{cstor}}) \tag{2}$$

$$f_2 = \mu_{\text{sol}} C_{\text{act}} S f_{\text{O2}} \tag{3}$$

$$f_3 = \mu_{\text{stor}} C_{\text{act}} f_{\text{cact}} f_{\text{O2}} \tag{4}$$

$$f_4 = \text{bstor} C_{\text{act}} \frac{f_x}{f_x + k_{\text{cstor}}} \tag{5}$$

$$f_5 = \text{bci} C_{\text{act}} f_{\text{O2}} \tag{6}$$

where bsstor = rate coefficient for soluble substrate conversion to stored mass (L/mg h); C_{act} = active mass concentration (mg/L); S = soluble substrate concentration (mg/L); f_{cstor} = fraction of volatile matter that is stored mass (mg/mg); f_{cstorm} = maximum possible value of fcstor (mg/mg); μ_{sol} = rate coefficient for soluble substrate conversion to active mass (L/mg h); f_{O2} = DO-limited reaction fraction; μ_{stor} = rate coefficient for stored mass conversion to active mass (h^{-1}); f_{cact} = manipulated fraction between stored mass and volatile matters; bstor = rate coefficient for particulate substrate conversion to stored mass (h^{-1}); f_x = fraction of sum of stored substrate and active mass that is stored substrate (mg/mg); k_{cstor} = half saturation coefficient, dimensionless (mg/mg); and bci = rate coefficient for active mass (h^{-1}).

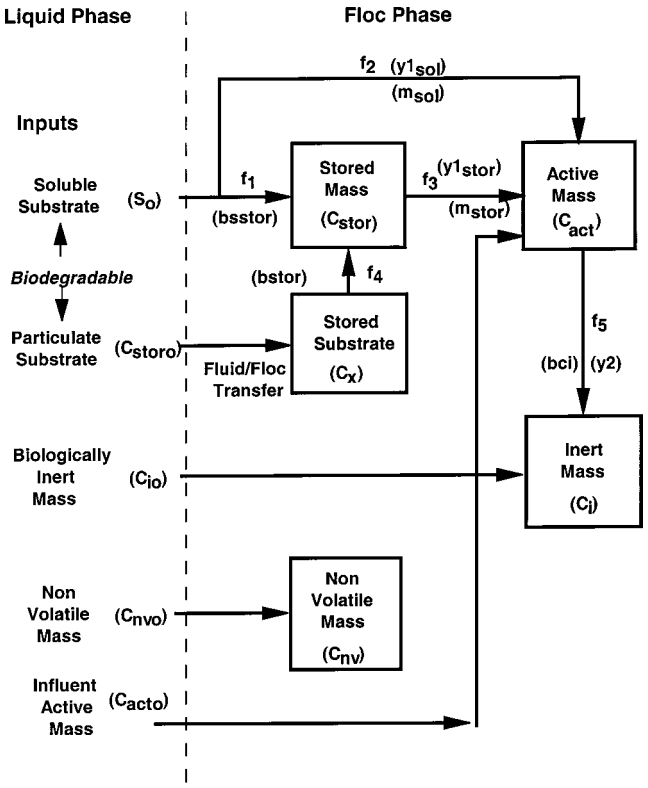

Fig. 2. Structured biological model schematic

The fraction functions contained in Eqs. (2)–(6) are described as follows:

$$f_{\text{O2}} = \frac{\text{DO}}{\text{DO} + K_{\text{SDO}}} \tag{7}$$

$$f_{\text{cstor}} = \frac{C_{\text{stor}}}{C_{\text{stor}} + C_{\text{act}} + C_{\text{i}}} \tag{8}$$

$$f_{\text{cact}} = \frac{f_{\text{cstor}}}{f_{\text{cstor}} + 1} \tag{9}$$

$$f_x = \frac{C_x}{C_x + C_{\text{act}}} \tag{10}$$

where K_{SDO} = DO half-velocity saturation coefficient (mg/L); C_{stor} = stored mass concentration (mg/L); C_i = inert mass concentration (mg/L); and C_x = stored (particulate) substrate concentration (mg/L).

Eq. (7) incorporates the impact of low DO concentration. The DO concentration in the HPO-AS process is typically higher than found in the AS process. McWhirter and Vahldieck (1978) suggested that the DO concentration needs to be 20% or more of the soluble substrate concentration to avoid DO limiting conditions, and generally recommended 6 mg/L.

Gas–Liquid Interactions

The liquid and gas phases in the HPO-AS process have different reactions occurring separately, and are combined through gas–liquid interactions (the gas transfer kinetics). The two-resistance

theory is used to describe the transfer, and Stenstrom et al. (1989) previously described the gas–liquid interactions and mass balances. Oxygen, carbon dioxide, and nitrogen are modeled. It is necessary to model the nitrogen because the influent wastewater will be saturated with dissolved nitrogen (the recycle sludge flow may or may not be saturated with nitrogen, depending upon site specific conditions). Atmospheric argon is modeled as nitrogen. Water vapor in the gas phase is important and can displace as much as 3% of the oxygen; water vapor is assumed to be saturated at the mixed-liquor temperature. Oxygen consumption is described as follows:

$$O_{2\text{Uptake}} = f_2\left(\frac{1-Y_{\text{sol}}}{Y_{\text{sol}}}\right)K_{\text{O2Sol}} + f_3\left(\frac{1-Y_{\text{Stor}}}{Y_{\text{Stor}}}\right)K_{\text{O2Stor}} + f_5(1-Y_2)K_{\text{O2ex}} \quad (11)$$

where Y_{sol}, Y_{Stor}, and Y_2 = yield coefficients for growth on soluble substrate, stored mass, and active mass decay, respectively; and K_{O2Sol}, K_{O2Stor}, and K_{o2ex} = stoichiometric coefficients with units of mass oxygen per mass of the appropriate substrate or cell mass. These coefficients are equal to 1 *if* substrates and cells are defined as chemical oxygen demand (COD).

The gas phase of each stage is assumed to be completely mixed. No gas back flow is allowed and no reactions occur in the gas phase. Gas leakage occurs with most HPO-AS systems, and is proportional to system pressure. System pressure is very nearly atmospheric, since the aeration tanks cannot be constructed as pressure vessels. Typical gas pressure in stage 1 is only 1.0074 Pa (75 mm water column gauge pressure), and decreases to 1.0025 (25 mm water column gauge pressure) in stage 4. Typical leakages are less than 5% of influent oxygen flow.

Secondary Clarifier

In order to simulate changing flow rate and other transient conditions, it is necessary to include a dynamic clarifier model into the plant model. The Bryant/Stenstrom one-dimensional model (Bryant 1972; Stenstrom 1976) divides the clarifier depth into several (normally ten) layers of equal height and calculates the settling flux of each layer according to an empirical settling velocity equation, a temperature correction factor, and the solid concentrations in the layer. The continuity from the surface layer to the bottom layer of the clarifier can predict the return sludge concentration accurately. Eq. (12) is the continuity or mass balance equation.

$$\frac{\partial C}{\partial t} = -(Vs+U)\frac{\partial C}{\partial Z} - C\frac{\partial Vs}{\partial Z} \quad (12)$$

where C = solids concentration; Vs = settling velocity of the solids relative to the liquid; U = downward or bulk velocity due to the sludge recycle; and Z = vertical clarifier dimension. Vs is a function only of solids concentration and temperature. By using finite differences, Eq. (12) can be written as follows:

$$\frac{dC_i}{dt} = \frac{U(C_{i-1}-C_i) + (Vs_{i-1}C_{i-1} - Vs_iC_i)}{\Delta Z} \quad (13)$$

where i denotes the layer, and ΔZ = thickness of layer i. The settling flux is defined as

$$Gs_i = Vs_iC_i \quad (14)$$

Several options of the settling function, Vs, are available. The key to making Eq. (13) accurately predict observed concentration profiles is to implement a flux constraint. The flux constraint states that the settling flux into layer i can be no larger than the settling flux that can be transmitted by layer i. Eq. (13) is written with the flux constraint as follows:

$$\frac{dC_i}{dt} = \frac{U(C_{i-1}-C_i)}{\Delta Z} + \frac{\text{Min}(Gs_i, Gs_{i-1}) - \text{Min}(Gs_i, Gs_{i+1})}{\Delta Z} \quad (15)$$

where Min = function that equals the lesser of its two arguments.

The top boundary condition is defined by the flow to the clarifier as follows:

$$\frac{dC_1}{dt} = \frac{\frac{Q(\text{MLSS}-Ce)+Qr\text{MLSS}}{\text{Area}} - UC_1 - \text{Min}(Gs_1, Gs_2)}{\Delta Z} \quad (16)$$

where Area = area of the clarifier; Q and Qr = influent and sludge recycle flow rates; Ce = clarifier effluent suspended solids concentration, and MLSS = mixed liquor total solids concentration. The settling flux is zero in the bottom element, and Eq. (15) becomes

$$\frac{dC_n}{dt} = \frac{U(C_{n-1}-C_n) + \text{Min}(Gs_n, Gs_{n-1})}{\Delta Z} \quad (17)$$

where n = index of the bottom element. This model predicts sludge accumulation in the clarifier and will predict failure as well. Failure is defined when the thick blanket reaches the top element, or a predefined, upper element. The value of Ce is changed to account for the dramatic increase in effluent solids. All categories of solids (particulate substrate, biologically inert mass, nonvolatile solids, etc.) have the same settling characteristics during the sedimentation process. Thus, the ratio among all categories of solids in the return sludge remains the same as in the influent to the clarifier.

The model, including gas phase interactions, requires the solution of 12 ordinary differential equations (ODEs) for each reactor stage. The secondary clarifier requires the solution of another set of ODEs equal in number to the number of elements. The series of ODEs can be solved by writing code in *FORTRAN 77*, as done herein, or another language, or using a simulation language such as *MatLab* or a similar program. The *FORTRAN* code has been extensively used on an IBM RISC 6000/390 workstation and PCs with Pentium processors. Typically, 1 or 2 min of computer time are required for each 100 h of simulated time. A more detailed description of the model and code development is available (Tzeng 1992).

Model Calibration

Calibration was performed using pilot plant data generated for the West Point Plant design. The pilot plant was operated with a steady-state influent flow rate of 144 m^3/day. Table 2 shows the operating data of the pilot plant (Samstag et al. 1989). The pilot plant was operated in step feed (sometimes called reaeration mode at HPO-AS plants) by feeding 100% of the influent flow to stage 2. The calibration procedure was similar to a sensitivity analysis. Typical values of the 13 kinetic coefficients (Grau et al. 1975; Metcalf and Eddy 1991) were first used to run the program with input data provided by the pilot study. Values of the influent flow rate and quality, the rate of HPO gas consumed, and the quantities of return flow and waste sludge were used. The output of the program was compared to the measured data. The first attempt gave high discrepancies. The next step was to either increase or decrease one of the 13 coefficients to see if the program gave better results.

Table 2. Calibrated Model Output Comparison to Pilot Plant Results

Parameter	Measured	Calibrated	Error (%)
OUR, stage 1 (mg/L-h)	63	65	3.2
OUR, stage 2 (mg/L-h)	96	91	5.2
OUR, stage 3 (mg/L-h)	49	51	4.1
OUR, stage 4 (mg/L-h)	41	35	14.6
MLVSS (mg/L)	1,171	1,169	0.20
MLSS (mg/L)	1,346	1,309	2.7
RAS MLVSS (mg/L)	3,112	3,207	3.1
RAS MLSS (mg/L)	3,577	3,593	0.40
O_2 consumption (kgO_2/kg BOD_{5R})[a]	0.52	0.49	5.8
Yield (kg VSS/kg BOD_{5R})	1.28	1.25	2.3
% O2, Stage 1	93.7	90.9	3.0
% O2, Stage 2	82.8	79.5	4.0
% O2, Stage 3	71.0	71.2	0.30
% O2, Stage 4	65.5	65.2	0.50

Note: OUR=Oxygen uptake rate

[a]BOD_{5R}=BOD_5 removed.

After several attempts of editing all of the 13 coefficients, a combination that has a good fit to the pilot-scale output was obtained. Table 3 gives the definitions and fitted values of the 13 coefficients. Table 2 also shows the model results and the error between the data and the model running with the coefficient values in Table 3. The percent errors show that except for oxygen uptake rate in stage 4, all other parameters give estimated values very close to the actual measured data. The average error for all 14 state variables is only 3.5%. The most useful parameters in this comparison table are the partial pressures of oxygen in each stage; it is easy to measure accurately and does not have high noise as a DO probe might have.

Plant Simulation

After calibration, it was possible to simulate the full-scale treatment plant design. This was viewed as an exercise to determine alternative ways to meet various process constraints, such as the required treatment capacities under different conditions. Mass transfer coefficients were not estimated in the pilot plant study. Therefore it was necessary to assume reasonable values for K_Las and α factors. The approximate K_La values were estimated from the power shown in Table 1 using Eq. (18) (Samstag et al. 1989)

$$K_La = 0.143 \cdot P^{0.9} \tag{18}$$

where P=stage propeller power in kW, and K_La is in units of h^{-1}. By assuming a mechanical/electrical efficiency of 75%, the designed powers can be converted to 4.14, 6.55, 6.55, and 4.14 h^{-1} for stage K_Las. These K_Las were used in developing Fig. 3. Performing clean water tests (ASCE 1991) would be more accurate, but was not necessary for this work. The α factors were assumed to equal 0.8 for all stages. These are higher than for submerged turbines (Stenstrom et al. 1989) which behave more like fine bubble devices, but are similar to α factors found at surface aerated HPO-AS plants (Whipple 1989).

Table 3. Fitted Model Parameters

Parameter	Value	Description and units
bci	0.005	decay coefficient (h^{-1})
Soluble BOD_5/BOD_u ratio	0.6	mg BOD_5/mgBOD_u
Particulate BOD_5/BOD_u ratio	0.55	mg BOD_5/mgBOD_u
bsstor	0.005	transfer coefficient (h^{-1})
bstor	0.6	transfer coefficient (h^{-1})
f_{cstrm}	0.3	maximum fraction (mg/mg)
K_{cstor}	0.05	saturation coefficient (mg/mg)
K_{SDO}	2.0	saturation coefficient (mg/L)
μ_{sol}	0.007	maximum growth rate (h^{-1})
μ_{stor}	0.750	maximum growth rate (h^{-1})
Y_{sol}	0.5	active mass yield (mg/mg)
Y_{stor}	0.55	active mass yield (mg/mg)
Y_2	0.05	inert mass yield (mg/mg)

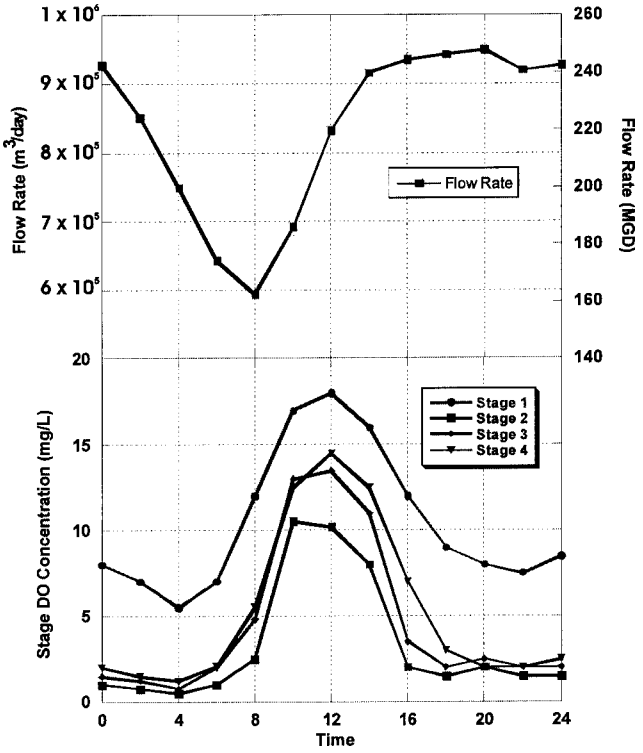

Fig. 3. Influent flow rate and uncontrolled dissolved oxygen response

Table 4. Process Loading Conditions

Flow condition	Flow rate m^3/day (MGD)	Primary eff. BOD_5 mg/L	Mass BOD_5 (tons/day)	Projected oxygen requirement (tons/day)	Projected oxygen consumption per unit of BOD_5 removed (kg/kg)[a]
Average annual day	542,000 (143)	91	49 (54)	63 (69)	1.2
Maximum month, average day	736,000 (195)	81	60 (66)	75 (83)	1.2
Maximum week, average day	1,130,000 (300)	61	69 (76)	88 (97)	1.2
Maximum day	1,130,000 (300)	87	99 (109)	120 (132)	1.1

[a]Estimated by assuming 95% BOD_5 removal and 90% oxygen utilization.

The first simulations were performed with the originally designed tank sizes and geometry (Table 1) and average influent condition, as shown in Table 4. These values are approximately equal to the early design conditions for the WPTP (Samstag et al. 1989). The influent flow rate varies diurnally as shown in Fig. 3 (top). This diurnal flow function was constructed using a function generator that connects observed flow rates in a piecewise linear fashion. The 24-h periodicity was repeated for as many days as the simulation ran. Fig. 3 (bottom) shows the uncontrolled stage DOs with the diurnal influent flow. These simulations do not use any control systems to modulate HPO gas feed or aerator speed to prevent high or low DO concentrations. Stage 1, which is used only for sludge reaeration, always has high DO. The lowest flow of 605,000 m^3/day (160 MGD) occurs at 8 a.m., and a peak of 960,000 m^3/day (255 MGD) occurs at 8 p.m. The DO concentrations show an inverse pattern as compared to the influent flow, and the minimum DO lags the maximum flow by 4 h. This inverse relationship is expected since less influent means that less oxygen is required for the oxidation reactions, and hence a higher DO concentration remains. The time lag reflects the simulation's ability to store substrates when the total amount of incoming BOD is high, and to use these stored materials when it is low.

The average DO over all four stages in Fig. 3 is 6 mg/L but the concentrations in stages 2, 3, and 4 fall far below the desired 6 mg/L set point for many hours of the day. Low DO concentration in HPO-AS plants for extended periods is generally believed to cause or contribute to filamentous sludge bulking. For DO concentrations less than 1.0 mg/L, bulking occurs whenever the g COD removed/g volatile suspended solids (VSS) ratio is greater than 0.45 (Palm et al. 1980). Therefore the performance of the aeration system is unacceptable. To avoid such problems, flow equalization or control systems must be used. The large tank volumes required for flow equalization are often prohibitive, and controls may be less expensive. Controls will usually produce energy savings.

To control DO, the operator or an automatic control device can be used to increase aerator K_La, by either increasing airflow rate in diffused air systems, or aerator revolutions per minute (rpm) or aerator propeller submergence in surface aerated systems. In HPO-AS plants, these options may be available, but an additional technique can also be used. It is possible to modulate the oxygen purities in each stage by changing the HPO gas flow to the aeration tanks. Increasing HPO gas flow is not without cost, since the higher gas flow rates require greater blower power at the oxygen production facility, and results in higher oxygen purity, even in stage 4, which decreases overall oxygen utilization efficiency. The gross oxygen consumption of the plant will increase when stage oxygen purities are increased. In this paper we compare the effectiveness of control strategies using 40, 50, and 60% stage 4 oxygen purities. Oxygen utilization decreases from a high of 90% utilized with 40% stage 4 purity, to 70% or less utilized with 60% stage 4 purity.

Control Strategies

In many HPO-AS designs, HPO feed gas is controlled using a pressure signal from stage 1. Since the absorption of oxygen is greater than the stripping of CO_2 and nitrogen, oxygen uptake decreases headspace pressure. This relationship has been used with success at some plants to maintain proper HPO gas feed rate. Stage 1 set point pressure can be maintained by a proportional-integral derivative (PID) or similar controller. Unfortunately, many plants have experienced problems using this approach because of the difficulty in obtaining a ''clean'' pressure measurement. The gage pressure in stage 1 is only 0.008 Pa, which can be less than pressure transients created by surface aerator splash. As a result, many HPO-AS plants have abandoned this control strategy in favor of manual control. An additional disadvantage of pressure control is its imperfect relationship to oxygen partial pressure; the gas composition is not constant. At different conditions the gas, particularly in stage 4, will be composed of varying amounts of carbon dioxide and nitrogen. An advantage of using stage 1 pressure as a control signal is that it responds very fast. There is essentially no lag in the pressure changed in stage 1 caused by oxygen uptake in all four stages. If stage 4 purity is used as a signal, the control system must overcome the long lag in stage 4 purity response. The gas retention time for all four stages may be as long as 12–16 h, depending upon utilization rate. Increasing HPO gas flow rate very slowly impacts stage 4 purity, and it is easy for controllers to oscillate or ''hunt'' around the set point.

Fig. 4 shows three possible control strategies and how they can be combined to improve results. The loop at the bottom can sense DO concentration and modify aerator rpm to reduce or increase DO concentration (only shown in one stage for clarity). The two loops at the top both modify HPO gas feed rate to control gas purity. The leftmost loop senses stage 1 pressure; the loop on the right senses stage 4 purity. The loops can be used singly or in combination. In combination, the pressure set point for stage one is modified by the error in the purity of stage 4 as compared to a set point. If stage 1 pressure is used alone, stage 4 purity is ignored. If stage 4 purity is used alone, the pressure signal is ignored and the stage 4 purity signal is passed through to manipulate HPO gas feed rate.

In this paper, we simulate PID controls, but other techniques are possible and perhaps more desirable. The PID algorithm is defined by Eq. (19)

$$\text{Valve position} = \text{previous position}\left(1 + Gp\ \text{error} + Gi\int \text{error}\ \mathrm{d}t + Gd\frac{\mathrm{dError}}{\mathrm{d}t}\right) \tag{19}$$

where Gp, Gi, and Gd are proportional, integral, and derivative

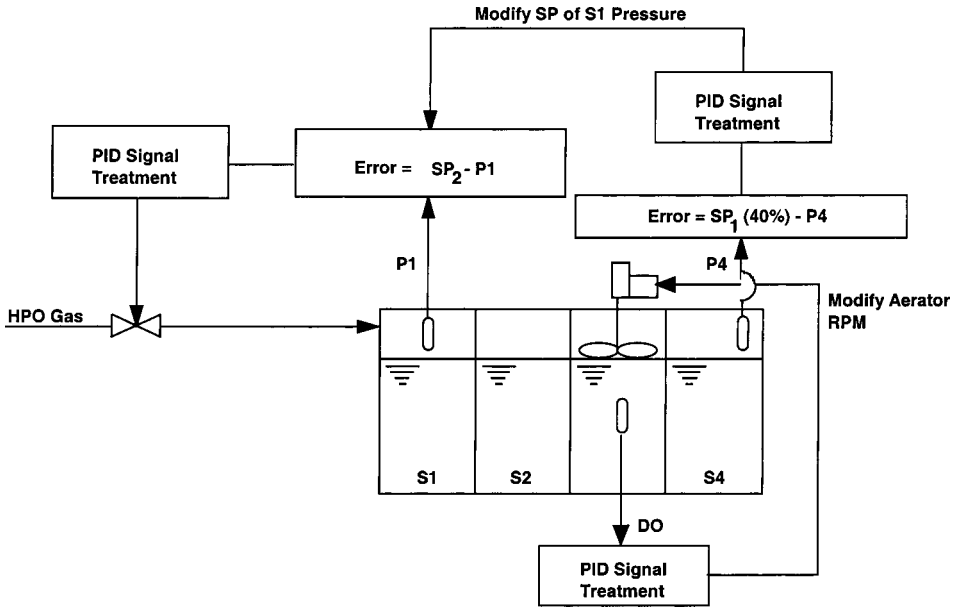

Fig. 4. Three control loops

gains, and Error is the difference between the process value and the set point. ''Valve position'' could be any manipulated parameter, such as aerator rpm or HPO valve opening.

The PID coefficients were optimized using a search algorithm. The influence coefficient method originally proposed by Becker and Yeh (1972) was adapted to determine optimum control coefficients by minimizing the integral of the squared error. This method can accommodate both explicit and implicit constraints. Error was defined as the difference between the set points and process value. In cases with multiple set points, such as the DO concentrations in each stage, the errors were added with equal weight. Tzeng (1992) describes the methodology. Yin and Stenstrom (1996) showed how fuzzy logic controls can be used in a similar fashion. The conventional methods used in this paper compare well for normal process disturbances. For extreme upsets, such as storm flow conditions, the fuzzy methods have better performance.

Most municipal plants are designed for some future capacity as well as peak flow loading conditions based upon season or diurnal flow rates. It is desirable to meet future conditions with minimum capital investment. Table 4 shows four different loading conditions for the WPTP: average annual day, maximum month average day, maximum week average day, and maximum day. The remainder of this paper shows how these various conditions can best be met using the three described control strategies.

Using the fixed K_Las associated with all flow conditions and fixed HPO gas flow rate, the range of DO concentrations in each stage are shown in Table 5. HPO gas flow was set to maintain an average stage 4 oxygen purity of 40, 50, or 60% for each condition; HPO gas feed rate was not changed to compensate for diurnal flow. The DOs in each stage are usually excessive (as compared to 6 mg/L), and energy is not conserved. Note how the HPO gas feed rate increases. These simulations create a set of base conditions to compare the effectiveness of the control strategies.

Vent Gas Purity Control

The two gas purity control strategies and the combined strategy were used optimized to control gas purity in stage 4. For pressure control strategy, stage 1 pressure set point was 1.008 Pa. The unoptimized system had a pressure variation of 1.00699–1.00910 Pa (70–90 mm water column gauge pressure). The optimized system had a pressure range of 1.0079–1.0080 Pa (83–84 mm water column gauge pressure). The pressure controller PID gains, as defined by Eq. (19), were 1,000 Pa^{-1}, 1,000 $Pa^{-1}\,h^{-1}$, and 300 h/Pa, respectively. Optimized purity ranged from 39.98 to 40.02%. The stage 4 purity PID gains were 500 (% oxygen)$^{-1}$, 500 (% oxygen h)$^{-1}$, and 100 h (% oxygen)$^{-1}$, respectively. The variations shown here are smaller than can be measured in the field. The combined method produced the most precise con-

Table 5. Comparison of Vent Purities and Oxygen Required with Different Purity Control Strategies

	No Vent Purity Control		Optimal Vent Purity Control		Optimal Vent Purity Control with DO Control	
Influent flow condition	Purity range (%)	HPO gas feed tons/day	Purity range (%)	HPO gas feed tons/day	Purity range (%)	HPO gas feed tons/day
Average annual day	37–53	62.8	40–40	58.3	40–40	53.3
Maximum month average day	39–54	79.3	40–40	71.3	40–40	64.3
Maximum week average day	36–51	88.4	40–40	85.0	40–40	77.4
Maximum day	38–54	119.7	40–40	108.8	40–40	105.3

trol, but at the expense of two simultaneous control loops. Using stage 4 purity alone in a single loop was successful but had greater tendency to oscillate with nonoptimal gains (results not shown).

Table 5 shows the results of using the combined loops. The uncontrolled case used the most oxygen and in the case of the average day, had vent purities ranging for a low of 37% to a high of 53%. For the combined stage 1 pressure with set point trim by stage 4 purity, the vent purity was constant at 40%, and required HPO gas decreased for all loading conditions by 4–10%. Set points of 50% and 60% stage 4 purity were also explored with similar results.

The final columns in Table 5 show the impact of operating vent purity controls with DO control (by assuming variable speed aerators, to be discussed more in the next section). Vent purity is again constant, and oxygen requirement decreased by 12–18% for the different loading conditions, as compared to the uncontrolled case. In the HPO-AS process, operating at excessive DO concentration has the traditional penalty of wasting aerator power, but has an additional penalty in that excessive DO in stage 4 is lost, and must be replaced by the oxygen generation plant. In conventional air AS, the aeration tank effluent DO is usually only 2 or 3 mg/L, but can be 10 mg/L or more in an HPO-AS process. Maintaining high aeration tank effluent DO has benefits, such as helping keep the clarifiers aerobic, but DO as high as 10 mg/L is probably wasted. Gas transfer in HPO plants includes two cost components: the cost for transfer, which is analogous to air AS processes, but also the cost to generate it, which does not exist with air processes. Therefore it is especially important to control DO in stage 4.

Dissolved Oxygen Control

The DO control loops can be turned on and the interaction of DO and oxygen purity can be investigated. Variable aeration rate must be assumed and can be accomplished by variable frequency drives or varying liquid level with level sensitive surface aerators. Constraints are used to simulate the maximum aerator turn-up or turn-down. Under constraints the controller will simulate the possible DO concentrations. If constraints are relaxed, essentially simulating an aerator without turn up or turn down limits, the simulation will calculate the $\alpha K_L a$s needed to maintain the set point DO for all conditions. A PID feedback DO controller was used.

Fig. 5 shows the required $\alpha K_L a$s without oxygen purity control. Each box represents one of the design conditions. The symbol in the middle of each bar represents the average value of $\alpha K_L a$. The upper and lower whiskers are the maximum and minimum values required to maintain 6 mg/L. Results for 40, 50, and 60% vent gas purities are shown. Fig. 6 shows the results but with optimal oxygen purity control loops turned on.

The required $\alpha K_L a$s without gas purity control are greater than with gas purity control. This occurs because the aerators do not have to contend with the reduced driving force that occurs with purity decline. For the uncontrolled case, the aerators in stages 2 and 4 are too small to avoid DO decline below 6 mg/L for the maximum day. Stage 4 is especially impacted. For the case with vent gas control, only stage 2 has insufficient transfer rate and it can be overcome by operating at higher vent purity. All are within the original design, except for stage 2 on the maximum day loading. Note that the required turn up and turn down is lower in all gas with vent purity control, which will reduce the cost and complexity of aerator design.

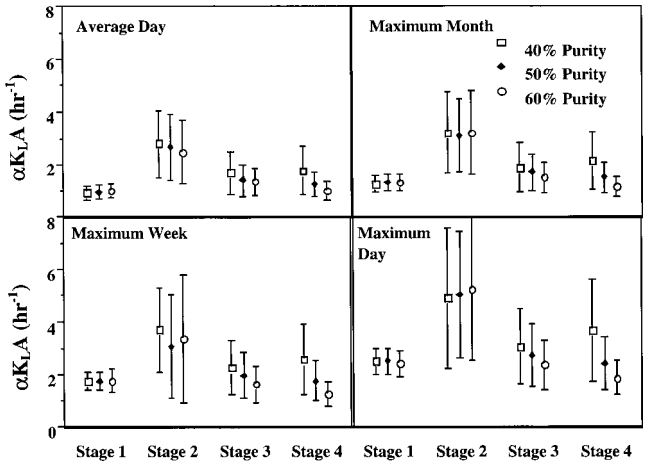

Fig. 5. Required $\alpha K_L a$ for each stage without oxygen purity control

Step Feed Operation

It is possible to balance DO by practicing step feed. In the previous examples, all the feed was applied to stage 2, turning stage 1 into a sludge reaeration reactor. It is possible to vary the feeding among the first three stages to balance oxygen demand. This method of operation was one of the original motivations for the development of step feed (Torpey 1948). Stenstrom and Andrews (1979) simulated controlling specific oxygen uptake rate in an activated sludge process by changing the distribution of feed between stages 1 and 2.

To determine the utility of this approach for an HPO-AS, feed distribution was distributed among the first three reactors with optimal vent gas purity control and DO control. Fig. 7 shows the required $\alpha K_L a$s to maintain 6 mg/L DO. As expected the $\alpha K_L a$s are smaller and the required turn up and turn down range is less. The average distribution among stages is 40, 26, and 34% to stages 1–3. The $\alpha K_L a$s are greatest in stage 3 due to the declining oxygen purity.

Cost Savings

The potential system savings of the combined control systems is large. For the maximum week condition using optimal purity and

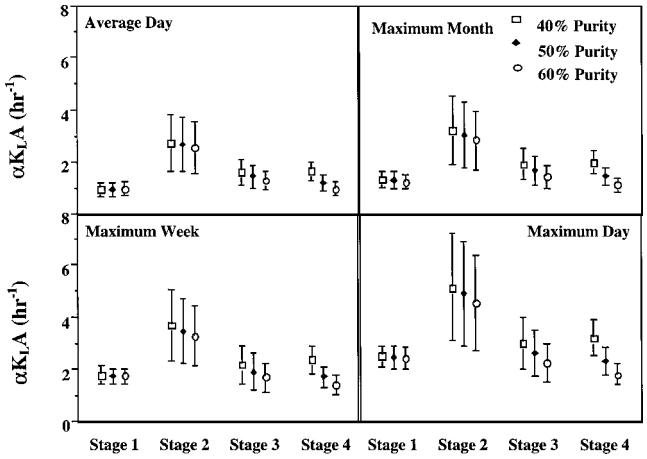

Fig. 6. Required $\alpha K_L a$ for each stage with optimal oxygen purity control

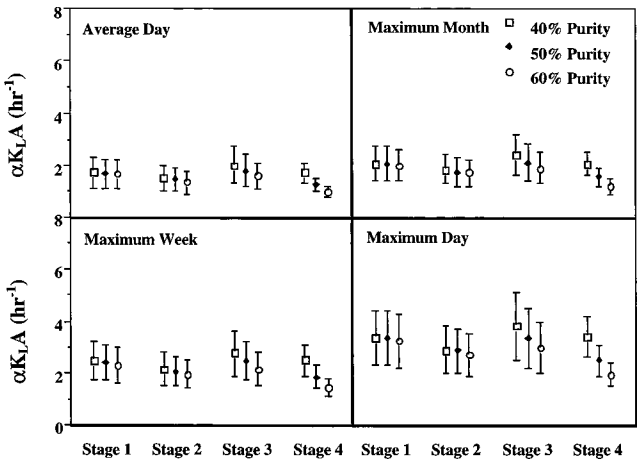

Fig. 7. Required $\alpha K_L a$ using step feed operation

DO control, the required aerator powers are 29, 98, 44, and 31 kW (38.7, 132, 59, and 40.8 horsepower) for stages 1–4. The total is 202 kW (270.5 h). As stated before, the design total power was 298 kW (400 h). The savings at \$0.10/kW h with six trains operating is \$505,000/year. The HPO gas savings varies among loading days, but was 24 tos/day for the average day condition (six trains operating). This savings, based on electricity cost for HPO gas production of \$20/ton (a survey of three California plants with average power cost of \$0.05/kW h) is \$175,000 per year.

Aeration costs at HPO-AS plants are now considered expensive in comparison to fine pore systems, which were generally not used in the U.S. during the development of the HPO-AS process (1970s). Poor gas utilization or high DO can cause these higher costs. As an example, compare a fine pore system in an air activated sludge process with standard aeration efficiency of 4.9 kg O2/kW h (8 lb O2/horsepower h) with a surface aerator HPO system with standard aeration efficiency of 1.95 kg O2/kW h (3.2 lb O2/horsepower h). Using a power weighted average HPO gas purity of 65%, alpha factors of 0.4 and 0.8 for fine pore and surface, respectively, and operating DOs of 2 and 6 mg/L for fine pore and surface, respectively, the HPO-AS system is slightly more expensive (6%) even if 100% HPO gas is utilized. These costs do not include any capital costs or other benefits. It is therefore very important to maintain high HPO gas utilization and operate at the minimum acceptable DO concentration.

Conclusions

This paper has investigated vent gas purity and DO control techniques for the high purity oxygen activated sludge process (HPO-AS). A structured biological model was used which was coupled with a gas phase model and a one-dimensional clarifier model. The model was calibrated with pilot plant data, and process sizes were selected that closely approximate an actual treatment plant. The simulation results show that it is possible to precisely control vent gas oxygen purity, which results in 4–10% reduction in oxygen feed, depending upon loading conditions. A two-loop controller was used, which adjusted feed gas rate primarily using stage 1 total pressure, with set point adjustment using stage 4 gas purity. With DO control, 12–18% savings in oxygen feed are realized. Dissolved oxygen control also reduces aerator power by approximately 30%. The simulations show that using step feed among the first three stages results in smaller variation aerator power and oxygen uptake rates. The other advantages of using step feed were not simulated, but should be similar to air activated sludge processes (Vitasovic and Andrews 1989).

References

American Society of Civil Engineers (ASCE). (1991). ''A standard for the measurement of oxygen transfer in clean water.'' ASCE-1984, New York.

Becker, L., and Yeh, W. W. (1972). ''Identification of parameters in unsteady open channel flows.'' *Water Resour. Res.*, 8(4), 956–965.

Bryant, R. (1972). ''Continuous time simulation of the conventional activated sludge wastewater renovation system.'' PhD dissertation, Clemson Univ., Clemson, S.C.

Busby, J. B., and Andrews, J. F. (1975). ''Dynamic modeling and control strategies for the activated sludge process.'' *J. Water Pollut. Control Fed.*, 47, 1055–1080.

Clifft, R. C. (1980). ''A dynamic model for predicting oxygen utilization in activated sludge processes.'' PhD dissertation, Univ. of Houston, Houston.

Clifft, R. C., and Andrews, J. F. (1986). ''Gas-liquid interactions in oxygen activated sludge.'' *J. Environ. Eng. Div. (Am. Soc. Civ. Eng.)*, 112(1), 61–77.

Clifft, R. C., and Barnett, M. W. (1988). ''Gas transfer kinetics in oxygen activated sludge.'' *J. Environ. Eng. Div. (Am. Soc. Civ. Eng.)*, 114(2), 415–432.

Grau, P., Dohanyos, M., and Chudoba, J. (1975). ''Kinetics of multicomponent substrate removal by activated sludge.'' *Water Res.*, 9, 637–642.

Heukelekian, H. (1941). ''Mechanical flocculation and bioflocculation of sewage.'' *Sewage Works J.*, 13(3), 506–522.

Hsieh, C. C., Babcock, R. W., and Stenstrom, M. K. (1993a). ''Estimating emissions of 20 VOCs. II: Diffused aeration.'' *J. Environ. Eng. Div. (Am. Soc. Civ. Eng.)*, 119(6), 1099–1118.

Hsieh, C. C., Ro, K. S., and Stenstrom, M. K. (1993b). ''Estimating emissions of 20 VOCs. I: Surface aeration.'' *J. Environ. Eng. Div. (Am. Soc. Civ. Eng.)*, 119(6), 1077–1098.

IAWPRC (1986). Activated Sludge Model No. 1, *Scientific and technical rep. No. 1*, IAWPRC, Queen Anne's Gate, London.

Jacquart, J. C., Lefort, D., and Rovel, J. M. (1972). ''An attempt to take account of biological storage in the mathematical analysis of activated sludge behavior.'' *Advances in water pollution research*, S. H. Jenkins, ed., Pergamon, New York, 367–372.

Linden, R. (1979). ''Model for minimizing energy requirements in the pure oxygen activated sludge process.'' PhD dissertation, Univ. of California, Davis, Calif.

McWhirter, J. R., and Vahldieck, N. P. (1978). *Oxygenation systems mass transfer design considerations. In the use of high-purity oxygen in the activated sludge process*, J. R. McWhirter, ed., Vol. 1, Chemical Rubber Corp., West Palm Beach, Fla., 235–260.

Metcalf & Eddy, Inc. (1991). *Wastewater engineering: treatment, disposal, and reuse*, 3rd Ed., McGraw–Hill, New York.

Mueller, J. A., Mulligan, T. J., and Di Toro, D. M. (1973). ''Gas transfer kinetics of pure oxygen system.'' *J. Environ. Eng. Div. (Am. Soc. Civ. Eng.)*, 99(3), 269–282.

Palm, J. C., Jenkins, D., and Parker, D. S. (1980). ''Relationship between organic loading, dissolved oxygen concentration and sludge settleability in the complete-mixed activated sludge process.'' *J. Water Pollut. Control Fed.*, 52, 2484–2506.

Samstag, R., et al. (1989). ''West Point treatment plant secondary treatment facilities—High purity oxygen design test facility draft report.'' *Seattle Metro*, Jan.

Stenstrom, M. K. (1976). ''A dynamic model and computer compatible control strategies for wastewater treatment plants.'' PhD dissertation, Clemson Univ., Clemson, S.C.

Stenstrom, M. K. (1990). ''Westpoint treatment plant oxygen process modeling.'' *Rep. No. UCLA-ENG 90-17*, 1–90.

Stenstrom, M. K., and Andrews, J. F. (1979). ''Real-time control of the activated sludge process.'' *J. Environ. Eng. Div. (Am. Soc. Civ. Eng.)*, 105(2), 245–260.

Stenstrom, M. K., Kido, W. H., Shanks, R. F., and Mulkerin, M. (1989). ''Estimating oxygen transfer capacity of a full scale pure oxygen activated sludge plant.'' *J. Water Pollut. Control Fed.*, 61, 208–220.

Torpey, W. N. (1948). ''Practical results of step aeration.'' *Sewage Works*, 20, 781–788.

Tzeng, C.-J. (1992). ''Advanced dynamic modeling of the high purity oxygen activated sludge process.'' PhD dissertation, Univ. of California, Los Angeles, Los Angeles.

Vitasovic, Z., and Andrews, J. F. (1989). ''Control systems for the activated sludge process, Parts I & II.'' *Water Pollution Research J. Canada*, 24(4), 479–496; 497–522.

Whipple, D. B. (1989). ''Dynamic modeling of the high purity oxygen activated sludge process.'' MS thesis, Univ. of California at Los Angeles, Los Angeles.

Yin, M. T., and Stenstrom, M. K. (1996). ''Fuzzy logic process control of the HPO-AS process.'' *J. Environ. Eng. Div. (Am. Soc. Civ. Eng.)*, 122(6), 484–492.

Yuan, W. (1994). ''Dynamic modeling and expert system for the activated sludge process.'' PhD dissertation, Univ. of California at Los Angeles, Los Angeles.

Yuan, W., Okrent, D., and Stenstrom, M. K. (1993). ''Model calibration for the high-purity oxygen activated sludge process – algorithm development and evaluation.'' *Water Sci. Technol.*, 28(11–12), 163–171.